ACCSCIENCE PUBLISHING

Journal of Seismic Exploration

ARTICLE

# Modeling the seismic wave equation using a staggered grid finite-difference method optimized with a genetic algorithm

**Mounika Vanga[1,2] and Maheswar Ojha[1,2]***

[1]CSIR – National Geophysical Research Institute, Uppal Road, Hyderabad-500007, Telangana, India

[2]Academy of Scientific and Innovative Research (AcSIR), Ghaziabad, Uttar Pradesh-201002, India

(This article belongs to the *Special Issue: Full Waveform Inversion Methods and Applications for Seismic Data in Complex Media*)

## Abstract

Simulation of seismic waves is a critical component in the imaging of subsurface structures using actual data, where numerical dispersion remains a challenging task. The finite-difference (FD) approach is popular for solving wave equations because it is simple to implement and requires less memory and computing time due to recursion. However, the staggered grid finite-difference (SGFD) methods have gained popularity due to their improved accuracy and stability. In this study, we introduce an optimization approach using a genetic algorithm (GA) to minimize numerical dispersion. The SGFD coefficients were optimized to reduce numerical errors and improve the accuracy of seismic wave simulations, considering both spatial and temporal domains. Numerical simulations applied to both homogeneous and heterogeneous velocity models demonstrate that the GA-optimized SGFD schemes achieve substantial reductions in dispersion, even with lower-order approximations, when compared to other methods. An important advantage of the proposed method is that it maintains high accuracy while using lower-order approximations, which significantly reduces computational costs. For example, the optimization of 12$^{th}$-order FD coefficients took approximately 20 s on a standard computer with 64 GB RAM. The findings demonstrate the efficiency of the proposed approach in improving the accuracy and stability of seismic wave simulations, providing a reliable solution for high-resolution seismic imaging.

***Keywords:*** Numerical dispersion; Seismic wavefield; Staggered grid finite-difference method; Genetic algorithm; Modeling; Optimization

***Corresponding author:**
Maheswar Ojha
(maheswarojha.ngri@csir.res.in)

**Citation:** Vanga M, Ojha M. Modeling of seismic wave equation using staggered grid finite-difference method, optimized by genetic algorithm. *J Seismic Explor*. doi: 10.36922/JSE025290035

**Received:** July 15, 2025

**Revised:** July 29, 2025

**Accepted:** July 30, 2025

**Published online:** August 20, 2025



## 1. Introduction

The numerical simulation of seismic waves has several applications in both applied seismic and seismology, and it is essential for understanding the Earth's subsurface structure. The finite-difference method (FDM) is one of the most popular techniques used to solve wave equations.[1-4] However, despite its popularity, the issue of numerical dispersion in simulating seismic waves remains a significant challenge. Numerical dispersion is a phenomenon that occurs in numerical simulations of wave propagation,

where the phase velocity depends on its wavelength and the discretization parameters of the numerical method. This leads to artificial distortion of the wave as it travels through the computational domain.

The numerical representation of a wave equation introduces errors that alter the phase velocity of the wave components. The causes of numerical dispersion include inadequate spatial or temporal resolution (i.e., large grid spacing or time steps), the choice of numerical scheme, and its truncation errors. Wave components with shorter wavelengths are more susceptible to numerical dispersion. The effects of dispersion may manifest as waves appearing to travel at incorrect speeds, smearing, or degraded modeling accuracy. Numerical dispersion is analyzed through the dispersion relation, which relates the numerical wavenumber to the physical wavenumber.

Alternative numerical approaches, including the Finite Element Method[5-9] and Finite Volume Method,[10-12] can be employed. Moreover, different grid schemes—such as conventional grid, staggered grid, variable grid, irregular grid—and various explicit and implicit formulas, offer further alternatives for numerical modeling. Staggered grid finite-difference (SGFD) methods, in particular, have gained prominence due to their enhanced accuracy and stability compared to conventional grid FDMs. The key distinction in SGFD methods is the utilization of first-order stress and strain relations instead of the direct second-order displacement relations. This approach not only increases accuracy but also leads to faster convergence[13] by reducing interpolation errors.

In general, finite-difference (FD) coefficients are determined through two main approaches: Taylor series expansion and optimization. Taylor series expansion involves representing functions as polynomials and estimating FD coefficients by comparing the coefficients of the polynomial dispersion relation equations.[14-17] Optimization methods[18-23] seek to minimize the dispersion error using techniques such as least squares, simulated annealing, and the sampling approximation method.[24] Recent studies also explore reducing dispersion at low wavenumbers using Lagrange dual problems[25] and explicit methods with optimized constant coefficients.[26]

Conventionally, SGFD coefficients are calculated in the space domain, but the dispersion relation depends on both space and time domains. Therefore, to achieve greater accuracy at designated frequencies, it is necessary to consider both domains.[14] A recent study[4] proposed an optimized FDM that minimizes dispersion by deriving explicit (conventional grid) FD coefficients using a genetic algorithm (GA). This method uses the combined time and space dispersion relation to compute FD coefficients adaptively based on parameters such as velocity, grid size, and time sampling to achieve greater accuracy.

SGFD methods have several advantages over conventional grid FDMs. SGFD methods can handle a wider range of grid geometries and boundary conditions than conventional grid methods. They are less constrained by Courant number limitations, which can significantly reduce computing time by allowing the use of greater time steps without compromising stability. In addition, SGFD methods are well-suited to optimization techniques. Improved results can be obtained by further minimizing numerical dispersion through the optimization of FD coefficients.

We implemented an approach to solve the wave equation using SGFD with GA, aiming to decrease numerical dispersion and computation time. The SGFD coefficients were derived from a dispersion relation by considering both time and space, using plane wave theory. The normalized phase velocity was used as the objective function in our optimization approach, which considers all pertinent variables such as velocity, grid size, and time step.

## 2. Methodology

### 2.1. FD coefficients through conventional methods

The 1D acoustic wave equation can be expressed as[27]:

$$\frac{1}{M'}\frac{\partial^2 u}{\partial t^2}=\left(\frac{\partial}{\partial x}\left(\frac{1}{\rho}\frac{\partial u}{\partial x}\right)\right)+s(t) \tag{1}$$

where $\rho$ is the density; $s(t)$ is the source field; and $M'$ is the P-wave modulus, given by $M'=\lambda+2\mu=\rho v^2$, where $\lambda$ and $\mu$ are the lame constants, $v$ is the velocity, and is the pressure field.

The $2M^{th}$ order SGFD formula for calculating the first-order derivatives is expressed as:

$$\frac{\partial u}{\partial x}=\frac{1}{\Delta x}\sum_{i=1}^{M}a_i\left(u^0_{i+\frac{1}{2}}-u^0_{i-\frac{1}{2}}\right) \tag{2}$$

where $u_i^j=u\left(x+i\Delta x,t+j\Delta t\right)$; $x$ and $t$ are the spatial and temporal coordinates; $\Delta x$ and $\Delta t$ are the grid spacing and time step, respectively; $i$ and $j$ are the spatial and temporal indices, and $a_i$ is the $i^{\text{th}}$ FD coefficient.

The second-order FD time derivative is used as:

$$\frac{\partial^2 u}{\partial t^2}=\frac{1}{\Delta t^2}\left(u_0^1-2u_0^0+u_0^{-1}\right) \tag{3}$$

where $u_0^0$ is the pressure field at the point $(x,t)$; $u_0^1$ is at the future time step $(x,t+\mathrm{j}\Delta t)$; and $u_0^{-1}$ is at the past time step $(x,t-\mathrm{j}\Delta t)$.

Using this second-order time derivative and the 2M[th] order spatial derivatives, the wave equation is expressed as:

$$\frac{1}{\Delta x^2}\sum_{i=1}^{M}\sum_{j=1}^{M}a_i a_j\left(\left(u_{i+j-1}^0-u_{i-1}^0\right)-\left(u_{-i+j}^0-u_{-i-j+1}^0\right)\right)$$
$$=\frac{1}{v^2\Delta t^2}\left(u_0^1-2u_0^0+u_0^{-1}\right) \quad (4)$$

where $a_i$ *and* $a_j$ are the coefficients.

By considering plane wave theory, the wave equation is expressed as:

$$u_i^j=e^{\iota\left(k(x+i\Delta x)-\omega(t+j\Delta t)\right)} \quad (5)$$

where $k$ is the wavenumber, $\omega$ is the angular frequency, and $\iota=\sqrt{-1}$ .

Substituting Equation (5) into the spatial derivative term Equation (2), the wavenumber is written as:

$$k\approx\frac{2}{\Delta x}\sum_{i=1}^{M}a_i\sin\left(\left(i-\frac{1}{2}\right)k\Delta x\right) \quad (6)$$

Using Taylor series expansion, the wavenumber is written as:

$$k\approx\frac{2}{\Delta x}\sum_{i=1}^{M}a_i\sum_{j=1}^{\infty}\frac{\sin\left(\left(i-\frac{1}{2}\right)k\Delta x\right)}{(2j-1)!} \quad (7)$$

$$\approx\frac{2}{\Delta x}\sum_{i=1}^{M}a_i\sum_{j=1}^{\infty}\frac{(-1)^{j-1}((i-0.5)\Delta xk)^{2j-1}}{(2j-1)!} \quad (8)$$

By comparing the coefficients of on both sides of Equation (8), we obtain the SGFD coefficients $a_1$, $a_2$,…$a_m$.

### 2.2. FD coefficients using both time and space domains

Liu and Sen[15] introduced an improved FDM by considering the joint time and space dispersion relation, ensuring better accuracy and stability. This method modifies the FD coefficients to satisfy the exact dispersion relation, thereby reducing errors in wave propagation.

By substituting Equation (5) into Equation (2), we obtain:

$$-\frac{4}{\Delta x^2}\sum_{i=1}^{M}a_i\sin\left((i-0.5)k\Delta x\right)\approx-\frac{4}{v^2\Delta t^2}\left[\sin(0.5vk\Delta t)\right]^2 \quad (9)$$

Using the sine function expansion, the coefficients for wave equation modeling are derived as:

$$a_i=\frac{(-1)^{i+1}}{2i-1}\prod_{1\le j\le M,\ i\ne j}\left|\frac{(2i-1)^2-(v\Delta t/\Delta x)^2}{(2i-1)^2-(2j-1)^2}\right| \quad (10)$$

### 2.3. FD coefficients through the optimization method

To minimize numerical dispersion and enhance accuracy, it is necessary to balance spatial and temporal discretization. Although refining the grid size and reducing the time step can improve accuracy, this significantly increases the computation time. An efficient alternative is to optimize FD coefficients by considering both spatial and temporal dispersion relations. Instead of relying solely on conventional Taylor series expansions, a GA can be employed to fine-tune FD coefficients. This approach reduces dispersion errors while maintaining computational efficiency, without the need for higher-order approximations, smaller grid sizes, or reduced time steps. GA, a global optimization method based on the theory of natural evolution, has been shown in previous studies to produce results that are equal to or better than those of simulated annealing[28] and to provide improved accuracy.[29] GA maintains a population of individuals, from which new generations are created through crossover and mutation operations. As the dispersion relation depends on both space and time, the phase velocity ratio was used as a fitness function for optimization. Over successive generations, the population evolves toward an optimal solution. The workflow for optimization is shown in Figure 1, and the steps for obtaining optimized FD coefficients are described below.

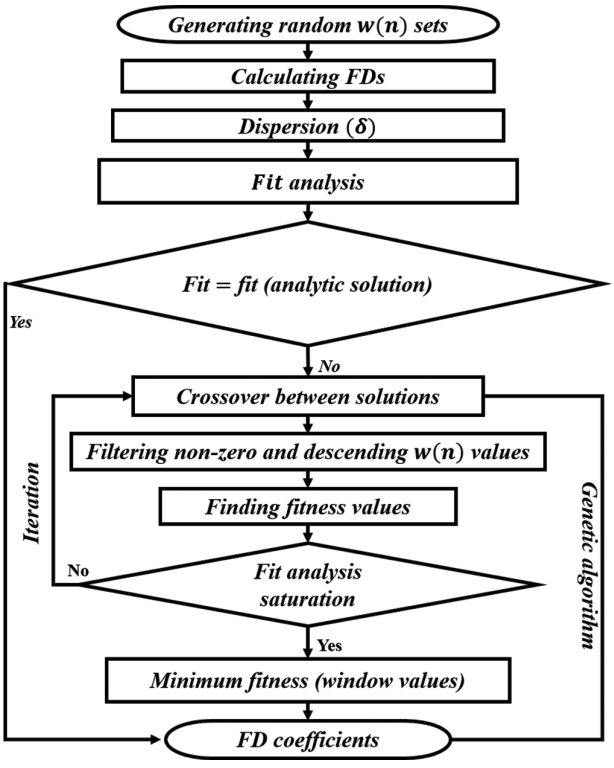


**Figure 1.** Workflow for optimization of finite-difference (FD) coefficients.

The sinc interpolation was used to derive the FD operator.[16] By applying the window values derived from this method, FD coefficients can be determined using Shannon's sampling theorem[30] as:

$$u(x)=\sum_{n=-\infty}^{\infty}\frac{\sin\frac{\pi}{\Delta x}(x-n\Delta x)}{\frac{\pi}{\Delta x}(x-n\Delta x)}u_n \tag{11}$$

The first derivative on a staggered grid was evaluated at midpoint $x=\frac{1}{2}\Delta x$, as follows:

$$\frac{\partial u}{\partial x}\Big|_{x=\frac{1}{2}\Delta x}=\frac{1}{\Delta x}\sum_{n=-\infty}^{\infty}\left\{-\frac{1}{\pi}\frac{\sin\left[(\frac{1}{2}-n)\pi\right]}{(\frac{1}{2}-n)^2}\right\}u_n \tag{12}$$

For a 2M-point SGFD operator approximation, Equation (12) becomes:

$$\frac{\partial u}{\partial x}\Big|_{x=\frac{1}{2}\Delta x}=\frac{1}{\Delta x}\sum_{n=1-M}^{M}w_n^M\left\{-\frac{1}{\pi}\frac{sin\left[(\frac{1}{2}-n)\pi\right]}{(\frac{1}{2}-n)^2}\right\}u_n \tag{13}$$

where $w_n^M$ are the window values.

The SGFD coefficients ($a_n$) were then determined from Equation (13) as:

$$a_n=-\frac{1}{\pi}\frac{\sin\left[\left(\frac{1}{2}-n\right)\pi\right]}{\left(\frac{1}{2}-n\right)^2}w_n^M,\qquad n=1-M,2-M,\ldots,M \tag{14}$$

In the optimization process, an initial population comprising numerous sets of random $M$ window values is generated for the 2$N$-order approximation, within the range of 0–1. Any number of initial sets can be considered; in this study, around 100 sets were used to ensure that the algorithm performs a global search. The FD coefficients are then computed using Equation (14). The phase velocity ratio (or dispersion relation) was used as the fitness function in GA.

The phase velocity ratio was calculated by substituting Equation (5) in Equation (4), expressed as:

$$\delta=\frac{2}{rk\Delta x}\sin^{-1}\left(r\sum_{m=1}^{M}a_m\sin\left[\left(\frac{2m-1}{2}\right)k\Delta x\right]\right) \tag{15}$$

where $r=\frac{v\Delta t}{\Delta x}$.

During each iteration process, crossover and mutation operations are applied to generate child populations of window values that better fit the fitness function. A weighted function was incorporated into the fitness function to minimize errors more effectively at low wavenumbers, as described by Vanga *et al.*[4] The final fitness function is given by:

$$fit=w_1err_{mean}+w_2err_{std} \tag{16}$$

where $w_1$ and $w_2$ are the weights assigned to the mean error ($err_{mean}$) and the standard deviation of the error ($err_{std}$), respectively, with the condition $w_1+w_2=1$. The mean error was calculated as:

$$err_{mean}=\frac{1}{\sum_{i=1}^{K}wg(i)}\sum_{i=1}^{K}wg(i)|1-\delta_i|$$

Where $wg(i)$ is the weighting function over $K$ samples, $K$ is the total number of wavenumber indices.

The standard deviation of the error is calculated as:

$$err_{std}=\sqrt{\frac{\sum_{i=1}^{K}[err(i)-err_{mean}]^2}{K}}$$

where $err(i)=|(1-\delta_i)|$ is the absolute error of the phase velocity ratio.

The weights $w_1$ and $w_2$ are user-defined parameters that determine the contribution of each error component to the final fitness value. In this study, different weighting functions were tested to identify the most suitable configuration.

## 3. Results

We tested linear, exponential, and cubic weighting functions by varying the weights used to calculate the mean dispersion error and standard deviation. After conducting several trials and evaluating the results, the linear weighting function $wg(i)=(k_{max}-i+1)$ was found to provide the best outcomes.[4] Based on this finding, we finalized the weight values as $w_1=0.8$ and $w_2=0.2$, which yielded optimal performance. These values are used in all subsequent numerical examples. We computed the FD coefficients derived using the GA and compared the resulting dispersion curves (phase velocity ratios), as shown in Figure 2, with those obtained using conventional and time-space Taylor series-derived FD coefficients.[15] These GA-derived solutions provide broader $kh$ coverage and show minimal frontal (time) dispersion, as the coefficients

are optimized considering both space and time domains. The proposed method achieves the accuracy of higher-order conventional and time-space methods even at lower orders (e.g., the proposed 8th-order method is equivalent to the 16th-order time-space and the 12th-order conventional method, as shown in Figure 2). The grid spacing is 10 m, the time step is 1 ms, and the wave propagation velocity is 2.5 km/s.

We also compared the results with the previously proposed GA-based explicit FD method,[4] as shown in Figure 3, which shows improved performance when using the staggered grid FDM over the explicit FDM.

To examine how dispersion varies with velocity for three different methods, we calculated phase velocity ratios (Figure 4) for wave velocities of 1.5 km/s (Figure 4A), 2.5 km/s (Figure 4B), and 4.5 km/s (Figure 4C), using

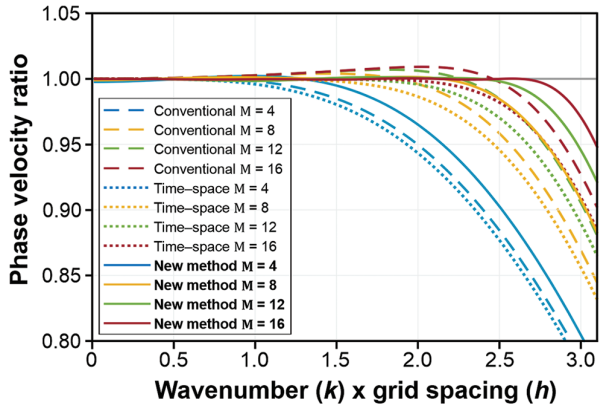


**Figure 2.** Plot of phase velocity ratio (dispersion) versus the product of the wavenumber ($k$) and grid spacing ($h$) for conventional, time-space and new genetic algorithm-based staggered grid methods, across various orders (M) of approximations.

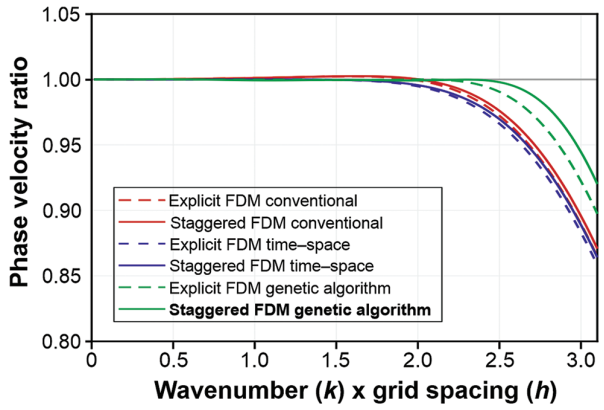


**Figure 3.** Dispersion curves versus $kh$ for conventional, time-space, and new genetic algorithm (GA)-based staggered grid finite-difference methods (FDM) compared with the GA-based explicit FDM for a 12th-order approximation.

4th, 8th, 12th, and 16th orders of approximation. As shown in Figure 4, it is observed that the new method produces significantly less dispersion compared to the conventional and time-space methods across all approximation orders and velocity settings.

Figure 5 shows the dispersion curves for different velocities using a 12th-order approximation for the conventional method (Figure 5A), the time-space method (Figure 5B), and the proposed method (Figure 5C). As shown in Figure 5A, it is clearly observed that, with increasing velocity, the conventional method exhibits high dispersion in both temporal and spatial components. In the case of the time-space method, temporal dispersion is eliminated; however, spatial dispersion remains significantly

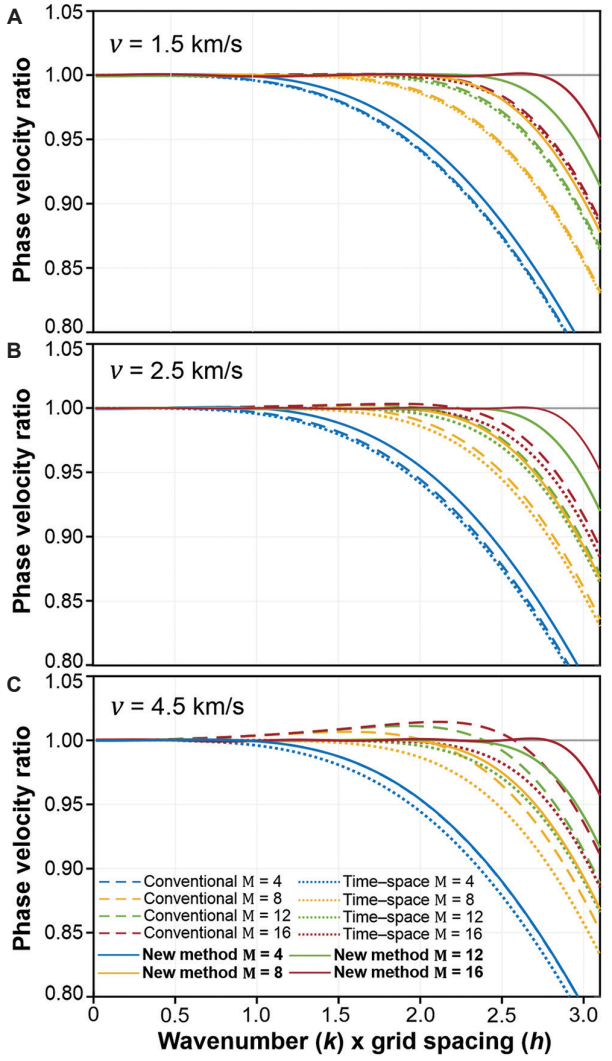


**Figure 4.** Dispersion versus the $kh$ for different velocities $v$: (A) 1.5 km/s, (B) 2.5 km/s, and (C) 4.5 km/s, for various order sof approximations $M$, using conventional, time-space, and new genetic algorithm-based staggered grid methods. The grid spacing is 15 m, and time step is 1 ms.

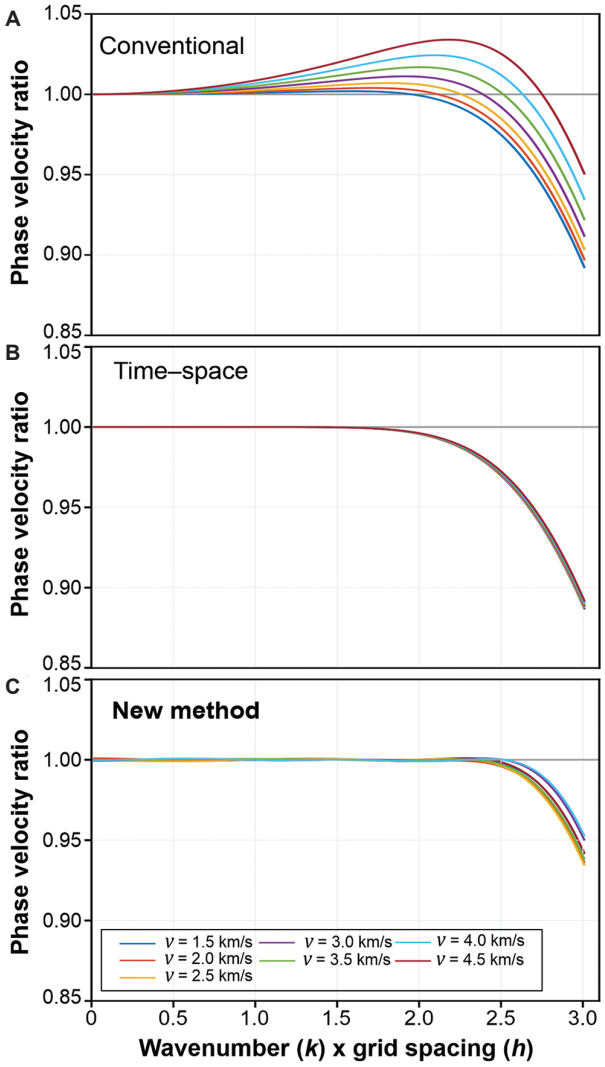


**Figure 5.** Dispersion versus *kh* for varying velocities *v*, using a 12th-order approximation for: (A) conventional, (B) time-space, and (C) new genetic algorithm-based staggered grid methods. Grid spacing is 10 m, and time step is 1 ms.

high at larger *kh* values compared to the proposed method. Although the time-space method exhibits stable dispersion behavior, it has limited wavenumber coverage. In contrast, the proposed method demonstrates greater stability and broader wavenumber coverage than both the conventional and time-space methods. The stability ratio (*s*) was calculated using the conventional eigenvalue method of stability analysis[15]:

$$s = \left( \sum_{m=1}^{M} a_m \right)^{-1}$$

Figure 6 shows the stability ratio as a function of increasing approximation order for the conventional, time-space, and proposed methods, using a velocity of 2.5 km/s, a time step of 1 ms, and a grid spacing of 15 m. It is also evident that the staggered FDM offers greater stability than the explicit FDM. SGFD methods are less constrained by Courant number limitations, which allows for the use of larger time steps without compromising stability. This, in turn, significantly reduces computation time.

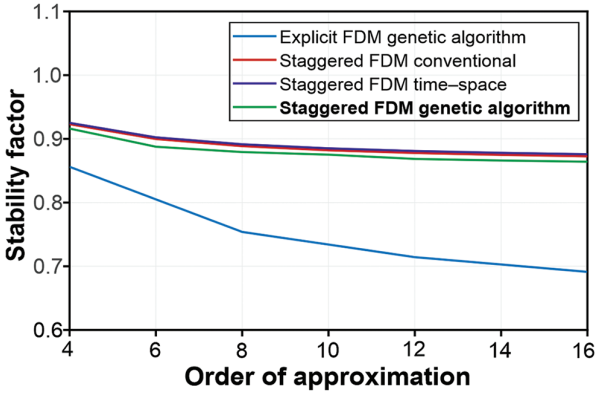


**Figure 6.** Comparison of stability conditions for the proposed genetic algorithm (GA)-based staggered grid finite-difference method (FDM; green) with the GA-based explicit FDM (blue), conventional staggered grid FDM (red), and time-space staggered grid FDM (purple).

### 3.1. Numerical examples of 2D wave propagation

For the 2D wave simulation, we consider three models: (i) a single velocity medium with 2.5 km/s, (ii) a horizontal-layered model, and (iii) the 2004 British Petroleum (BP) benchmark salt-dome model. We compared 2D wave propagation results at different simulation times using the conventional and time-space method for 4th, 8th, and 12th-order approximations. A 40th-order conventional method was used as the reference solution. Figure 7 presents 2D wave propagation snapshots for the single-velocity medium. Quarter I shows the reference solution using the 40th-order conventional method; quarter II displays results from the GA-based method; quarter III shows the conventional method; and quarter IV is the time-space method. Snapshots were taken at 0.5 s (top panel) and 1.15 s (bottom panel). The wavefields were generated in a single velocity (2.5 km/s) medium measuring 3 km × 3 km, using a grid spacing of 15 m, a time step 1 ms, and a 30 Hz Ricker wavelet as the source. The results show that the proposed GA-based method exhibits significantly lower dispersion across all snapshot times compared to other SGFD methods.

Figure 8 shows the horizontal-layered model (Figure 8A) and the 2004 BP benchmark salt-dome model[31] (Figure 8B), both used to generate synthetic shot gathers. To reduce computational cost, we used staggered FD

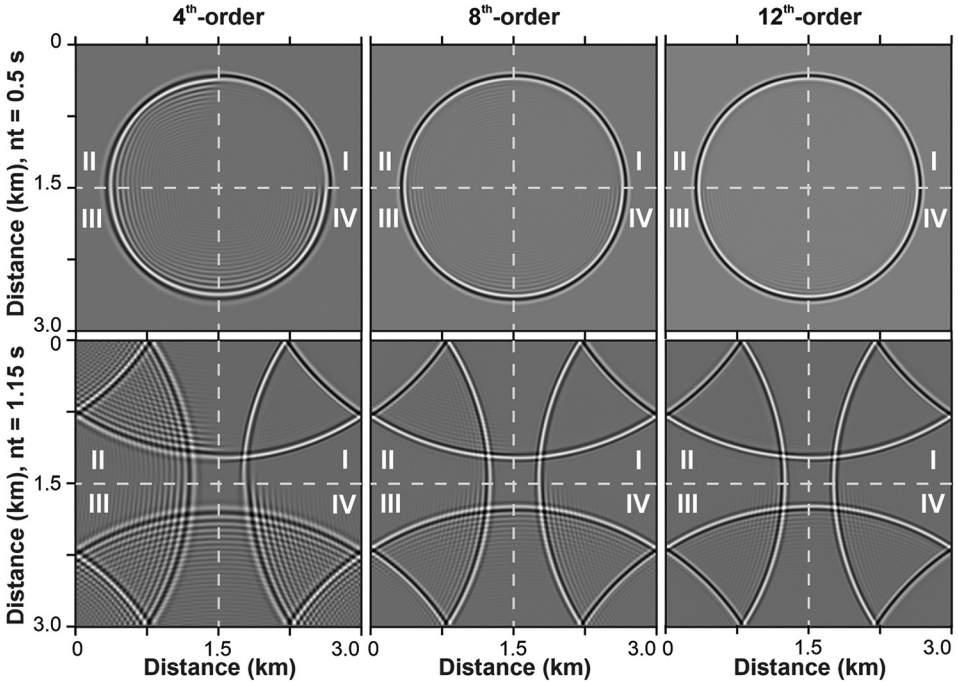


**Figure 7.** Snapshots of 2D wave propagation in a homogeneous model for 4th, 8th, and 12th orders. Quarter I shows the reference wavefield generated using the 40th-order conventional method; quarter II is the new genetic algorithm-based method; quarter III is the time-space method; and quarter IV is the conventional method.

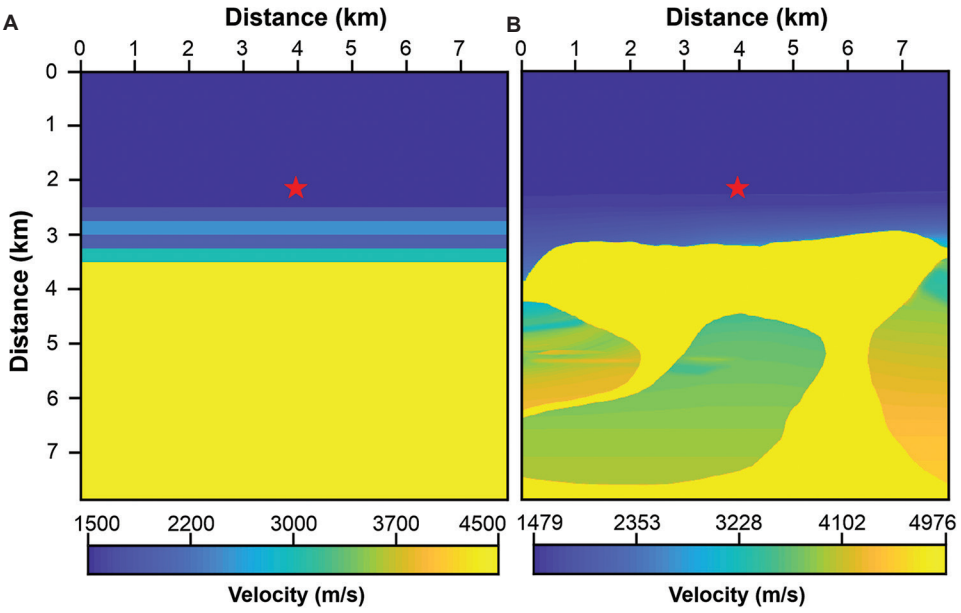


**Figure 8.** Velocity models used in the study: (A) the horizontal-layered model, and (B) the 2004 BP benchmark salt-dome model. Red stars indicate the source positions.

coefficients optimized for the minimum velocity in each model. Given that lower velocities (i.e., higher $kh$) are more dispersive and exhibit reduced wavenumber ($k$) coverage compared to higher velocities, coefficients optimized for the lowest velocity in the model can be applied effectively across the full velocity range. However, if the velocity range in the model is very broad, coefficients may need to be optimized for different velocity zones to achieve better

**Table 1. Optimized finite-difference coefficients for 12th-order approximation**

| Velocity (m/s) | Coefficient 1 | Coefficient 2 | Coefficient 3 | Coefficient 4 | Coefficient 5 | Coefficient 6 |
|---|---|---|---|---|---|---|
| 1,500 | 1.24712819 | −0.11964252 | 0.03317386 | −0.01119058 | 0.00340783 | −0.00058573 |
| 2,000 | 1.23966780 | −0.11480708 | 0.03063733 | −0.00987106 | 0.00270170 | −0.00024662 |
| 2,500 | 1.23345081 | −0.11135320 | 0.02889657 | −0.00883066 | 0.00214908 | −0.00018497 |
| 3,000 | 1.23220741 | −0.11342553 | 0.03262676 | −0.01146971 | 0.00397580 | −0.00101733 |
| 3,500 | 1.21853003 | −0.10458359 | 0.02795159 | −0.00870379 | 0.00224119 | −0.00036994 |
| 4,000 | 1.21355644 | −0.10444543 | 0.03043838 | −0.01101295 | 0.00394510 | −0.00101733 |
| 4,500 | 1.19863567 | −0.09518902 | 0.02546479 | −0.00804402 | 0.00217978 | −0.00033911 |

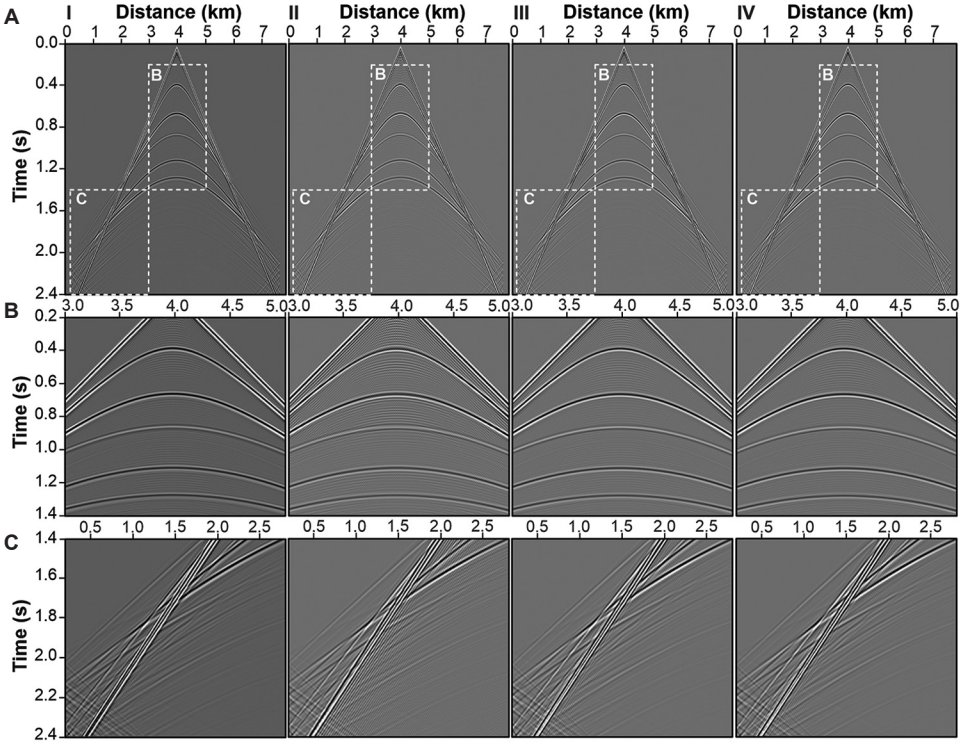


**Figure 9.** Shot gathers (A) for the horizontal-layered model (Figure 8A). (I) Reference gather generated using the 40th-order conventional method, (II) 12th-order conventional method, (III) new genetic algorithm (GA)-based method with finite-difference (FD) coefficients optimized for the lowest velocity in the model, and (IV) new GA-based method with varying FD coefficients optimized across a range of velocities. Zoomed-in views of the dashed white boxes (B and C) inside Figure A are shown below the corresponding gathers.

accuracy. The values of the optimized coefficients for a 12th-order approximation, using a grid size of 10 m and a time step of 1 ms, are provided in Table 1.

Figure 9 shows the shot gathers computed using the horizontal-layered model (Figure 8A) and Figure 10 shows the shot gathers generated from the BP 2004 benchmark salt-dome model (Figure 8B). The horizontal-layered model was used to interpret wave propagation without diffraction effects. The source was placed at $x$ = 3990 m and $z$ = 2250 m. We employed the first derivative of the staggered scheme to discretize the wave equation and used a time step $\Delta t$ = 1 *ms* and grid spacing $\Delta x$ = 10 m. Shot gathers were computed using both the conventional and GA-based methods. The gather generated using the 40th-order conventional method is considered the reference (Figures 9I and 10I). Figures 9(II) and 10(II) show the results for the 12th-order conventional method. Figures 9(III) and 10(III) present the new GA-based method using FD coefficients optimized with the lowest velocity in the model, while Figures 9(IV) and 10(IV) show the new GA-based method using FD coefficients optimized over a range of velocities. Compared to the conventional method, the GA-based optimized method yielded improved results with reduced dispersion and

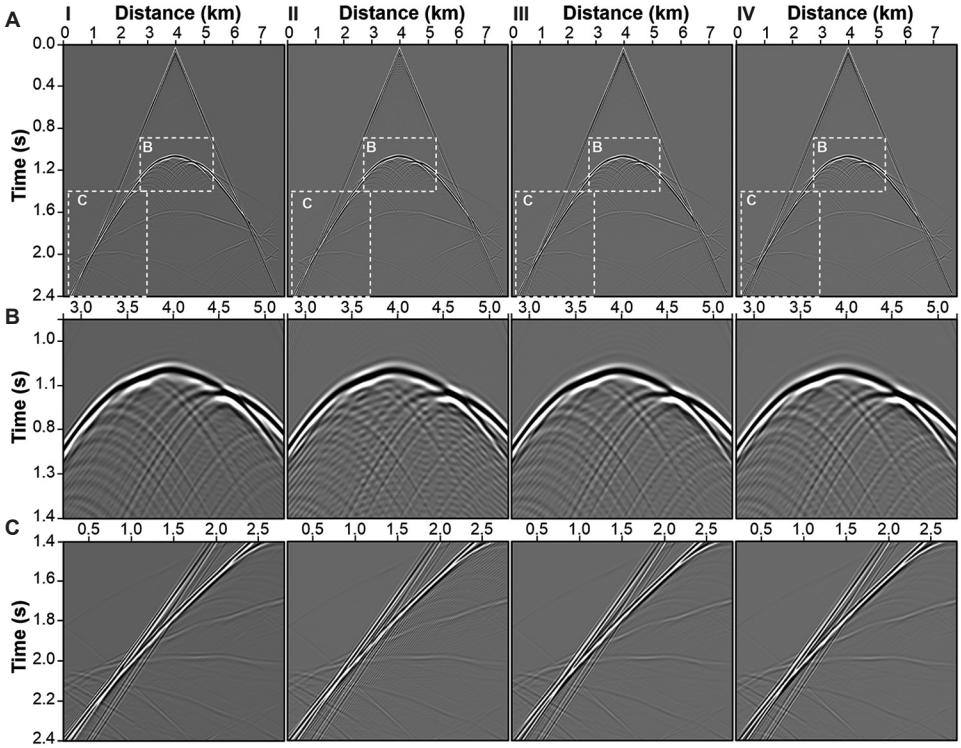


**Figure 10.** Shot gather (A) for the BP salt-dome model (Figure 8B). (I) Reference gather generated using the 40th-order conventional method, (II) 12th-order conventional method, (III) new genetic algorithm (GA)-based using finite-difference (FD) coefficients optimized for the lowest velocity in the model, and (IV) new GA-based method using varying FD coefficients optimized for a range of velocities. Zoomed-in views of the dashed white boxes (B, C) inside Figure A are shown below the corresponding gathers.

lower computational cost by using a lower-order expansion with optimized coefficients. Two optimization approaches were considered: Figures 9(III) and 10(III) show that FD coefficients were optimized using the lowest velocity in the model, while Figures 9(IV) and 10(IV) show that FD coefficients were optimized across a range of velocities. Specifically, SGFD coefficients were optimized at intervals of every 500 m/s. Figures 9(III) and 10(III) good balance between computational efficiency and accuracy, making it suitable for applications requiring broad adaptability across varying velocities. In contrast, as shown in Figures 9(IV) and 10(IV), though slightly more computationally intensive, provide enhanced accuracy in regions with sharp velocity contrasts or complex geological features. This approach is generally more effective in minimizing dispersion errors under varying velocity conditions, thereby improving the reliability of wave propagation simulations in challenging environments.

Numerical modeling using 12$^{th}$-order approximations of the GA-based, conventional and reference (40$^{th}$-order conventional) was performed. The simulated results are shown in Figures 11 and 12 for the horizontal-layered and salt-dome velocity models, respectively (Figure 8). Figures 11A and 12A present the reference wavefields generated using the 40$^{th}$ conventional method. Figures 11B and 12B correspond to the 12$^{th}$-order conventional method. Figures 11C and 12C show results from the proposed SGFD method using FD coefficients optimized for the minimum velocity in the model, while Figures 11D and 12D show the SGFD method using FD coefficients optimized over a range of velocities. In the horizontal-layered model, five interfaces are present, with the third interface being a negative interface. In the bottom panel of Figure 11, the first signal in the seismic traces corresponds to the direct wave; the second to the first interface; the third to the second interface; the fourth to the negative interface; the fifth to the fourth interface; and the sixth to the fifth interface. The 12$^{th}$-order conventional method shows more dispersion in all reflected signals (including direct and interface reflections), as observed in the seism mic traces beneath the snapshots. As shown in Figures 11 and 12, it is evident that the seismogram produced by the proposed method exhibits significantly less dispersion compared to the conventional method.

## 4. Discussion

This study focused on modeling seismic wave equations using the SGFD approach combined with GA optimization. The primary goals of seismic wave simulation are to reduce

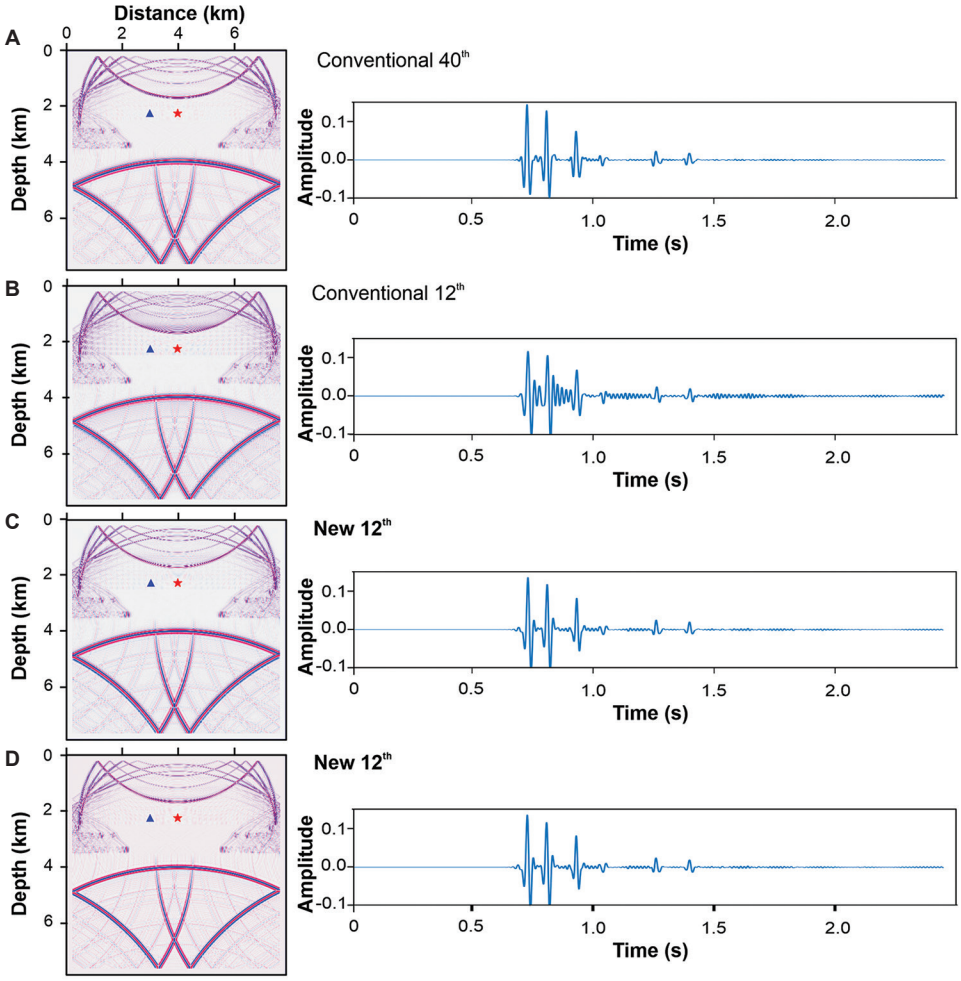


**Figure 11.** Acoustic wave simulations in the horizontal-layered model (Figure 8A). (A) Reference wavefield generated using the 40th-order conventional method. Wavefields generated using the 12th-order approximation for: (B) conventional and (C) new genetic algorithm (GA)-based method using finite-difference (FD) coefficients optimized for the minimum velocity, and (D) new GA-based staggered grid FD method with varying FD coefficients optimized for a range of velocities. Seismic traces shown below the wavefields correspond to the source (red stars) and receiver (blue triangles) locations.

numerical dispersion, improve accuracy, and minimize computational time. The staggered grid approach is preferred over conventional methods due to its inherent interpolation accuracy and stability. GA is employed to improve FD coefficients by considering velocity, grid spacing, and time step, resulting in coefficients that better satisfy both spatial and temporal dispersion relations. Even with lower-order approximations, the study demonstrates that GA-optimized coefficients outperform traditional and time-space Taylor series-derived coefficients by providing broader wavenumber coverage and reduced frontal dispersion.

The computation times for optimizing coefficients over 20 iterations using a standard workstation with 60 Gb RAM are 12.873, 21.390, 21. 993, and 22.064 s for the 4th, 8th, 10th, and 12th orders, respectively. The computational cost of optimizing FD coefficients using GA does not scale linearly with the order of approximation. While higher-order schemes, such as the 12th order, involve more coefficients than lower-order schemes like the 6th order, the increase in computation time is not directly proportional. This is because the solution space expands significantly at higher orders, providing more flexibility for GA to converge efficiently toward an optimal set of coefficients. As a result, although higher-order approximations require more iterations, the search benefits from a larger parameter space, leading to a more gradual increase in computation time rather than linear growth. There is some randomness in the values of each optimized coefficient during the GA process due to its stochastic nature. However, after a sufficient number of iterations, the overall accuracy and wavenumber coverage remain consistent. This ensures that variations in individual coefficients do not significantly affect the modeling outcomes.

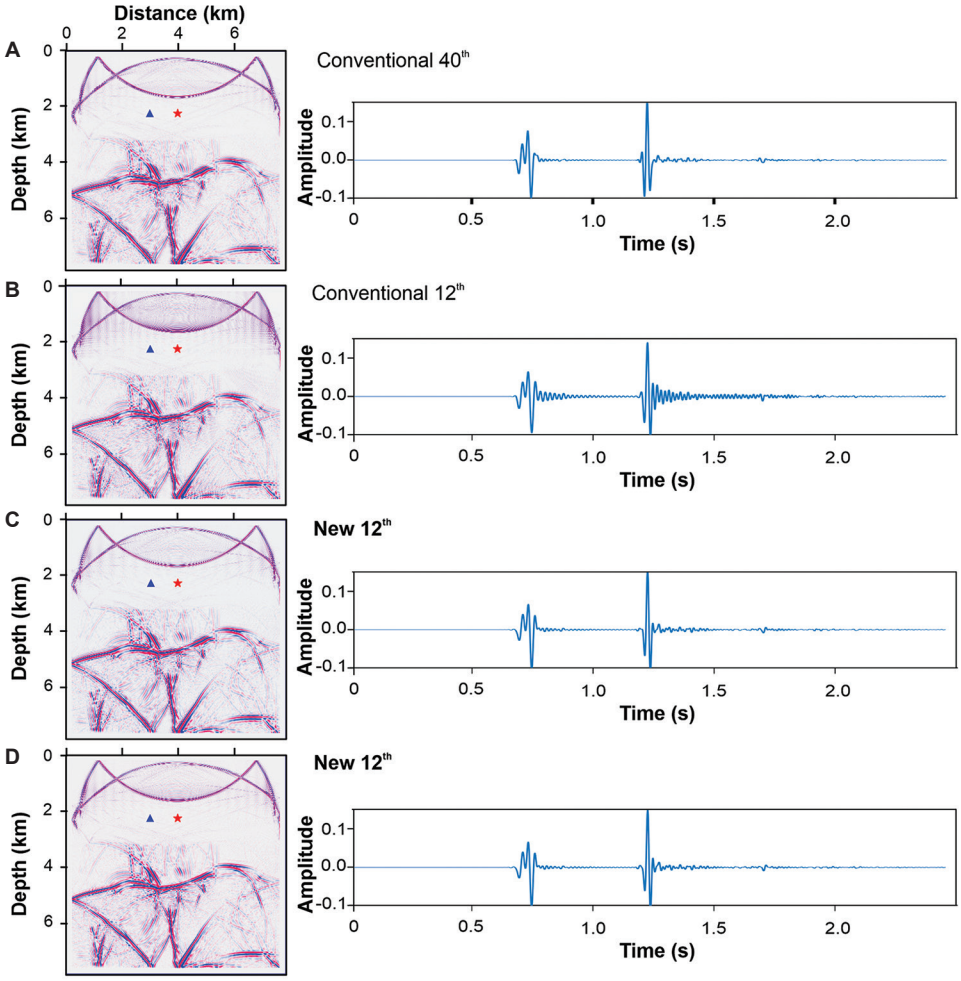


**Figure 12.** Acoustic wave simulations in the BP salt-dome model (Figure 8B). (A) Reference wavefield generated using the 40$^{th}$-order conventional method. Wavefields generated using the 12$^{th}$-order approximation for: (B) conventional, and (C) new genetic algorithm (GA)-based method using finite-difference (FD) coefficients optimized for the minimum velocity, and (D) new GA-based method with varying FD coefficients optimized for a range of velocities. Seismic traces shown below the wavefields were generated using the source and receiver locations indicated by red stars and blue triangles, respectively.

For wavefield simulation, the computation time for both the horizontal-layered and salt-dome model was approximately 110 s, as both models used the same grid size and simulation time (2.4 s). However, when using FD coefficients optimized across a range of velocities, the same simulations take about 130 s due to the additional computation required to apply multiple velocity-dependent stencils. These results show the adaptability of the method to complex structures and highlight how optimized FD coefficients can be reused across a range of velocities within a model. When modeling complex geological structures, velocity variations tend to increase. For such models, FD coefficients optimized across a range of velocities can be precomputed and stored them as stencils for future simulations, providing an efficient and flexible solution.

## 5. Conclusion

We propose an SGFD method for seismic wavefield simulation, in which the FD coefficients are optimized using a GA. Our results show improved accuracy and reduced numerical dispersion compared to both conventional and time-space methods. Although the computational cost for determining the optimized coefficients is higher than that of conventional methods, this is a 1-time expense. Once the algorithm is run for a set of representative velocities in the model and the optimal coefficients are obtained, the final simulation cost is reduced. This is because the proposed method achieves high accuracy even with lower-order approximations. For example, the eighth-order approximation using the proposed method provides results similar to the 12$^{th}$-order time-space method (Figure 2), and the 12$^{th}$-order approximation yields results comparable to

the 40th-order conventional method (Figures 11 and 12). The results presented in this study demonstrate that the optimized SGFD method can be effectively used for seismic wave simulation and may support comparison with real data to obtain more accurate subsurface imaging.

## Acknowledgments

The authors gratefully acknowledge the Council of Scientific and Industrial Research—National Geophysical Research Institute (CSIR-NGRI), Hyderabad, for providing academic guidance and research infrastructure. The authors also thank the Academy of Scientific and Innovative Research (AcSIR) for serving as the academic body facilitating the doctoral program and for their continuous support throughout this research.

## Funding

This research was supported by the Ministry of Earth Science (MoES), New Delhi (grant number: MoES/OSMART/EFC2021 - OM No. 01(01)/PFC-I/2022).

## Conflict of interest

The authors declare that they have no competing interests.

## Author contributions

*Conceptualization:* Mounika Vanga, Maheswar Ojha
*Formal analysis:* Mounika Vanga
*Investigation:* Mounika Vanga
*Methodology:* Mounika Vanga
*Software:* Mounika Vanga
*Writing–original draft:* Mounika Vanga
*Writing–review & editing:* Mounika Vanga, Maheswar Ojha

## Availability of data

No data is associated with this theoretical work.

## References

1. Kelly KR, Ward RW, Treitel S, Alford R. Synthetic seismograms: A finite -difference approach. *Geophysics*. 1976;41(1):2-27.

   doi: 10.1190/1.1440605.

2. Zhi-Yang W, Hong L, Xiang-De T, Yang W. Optimized finite-difference operator based on chebyshev auto-convolution combined window function. *Chin J Geophys*. 2015;58(2):192-206.

   doi: 10.1002/cjg2.20166

3. Jing H, Yang G, Wang J. An optimized time-space-domain finite difference method with piecewise constant interpolation coefficients for scalar wave propagation. *J Geophys Eng*. 2019L;16(2):309-324.

   doi: 10.1093/jge/gxz008

4. Vanga M, Barman D, Ojha M. An optimized finite difference method to minimize numerical dispersion of acoustic wave propagation using a genetic algorithm. *Geophysics*. 2022;87(3):T265-T279.

   doi: 10.1190/geo2021-0382.1

5. Patera AT. A spectral element method for fluid dynamics: Laminar flow in a channel expansion. *J Comput Phys*. 1984;54(3):468-488.

   doi: 10.1016/0021-9991(84)90128-1

6. Komatitsch D, Vilotte JP. The spectral element method: An efficient tool to simulate the seismic response of 2D and 3D geological structures. *Bull Seismol Soc Am*. 1998;88(2):368-392.

   doi: 10.1785/bssa0880020368

7. Chaljub E, Komatitsch D, Vilotte JP, Capdeville Y, Valette B, Festa G. Spectral-element analysis in seismology. *Adv Geophys*. 2007;48:365-419.

   doi: 10.1016/s0065-2687(06)48007-9

8. Cristini P, Komatitsch D. Some illustrative examples of the use of a spectral-element method in ocean acoustics. *J Acoust Soc Am*. 2012;131(3):EL229-EL235.

   doi: 10.1121/1.3682459

9. Bottero A, Cristini P, Komatitsch D, Asch M. An axisymmetric time-domain spectral-element method for full-wave simulations: Application to ocean acoustics. *J Acoust Soc Am*. 2016;140(5):3520-3530.

   doi: 10.1121/1.4965964

10. Dormy E, Tarantola A. Numerical simulation of elastic wave propagation using a finite volume method. *J Geophys Res Atmos*. 1995;100(B2):2123-2133.

    doi: 10.1029/94jb02648

11. Eymard R, Gallouët T, Herbin R. Finite volume methods. In: *Handbook of Numerical Analysis*. Amsterdam: Elsevier; 2000. p. 713-1018.

    doi: 10.1016/s1570-8659(00)07005-8

12. Komatitsch D, Erlebacher G, Göddeke D, Michéa D. High-order finite-element seismic wave propagation modeling with MPI on a large GPU cluster. *J Comput Phys*. 2010;229(20):7692-7714.

    doi: 10.1016/j.jcp.2010.06.024

13. Igel H, Riollet B, Mora P. *Accuracy of Staggered 3-D finite-Difference Grids for Anisotropic Wave Propagation*. Society of Exploration Geophysicists. 1992. p. 1244-1246.

    doi: 10.1190/1.1821960.

14. Finkelstein B, Kastner R. Finite difference time domain dispersion reduction schemes. *J Comput Phys*. 2006;221(1):422-438.

doi: 10.1016/j.jcp.2006.06.016

15. Liu Y, Sen MK. Scalar wave equation modeling with time-space domain dispersion-relation-based staggered-grid finite-difference schemes. *Bull Seismol Soc Am*. 2011;101(1):141-159.

doi: 10.1785/0120100041

16. Chu C, Stoffa PL. Determination of finite-difference weights using scaled binomial windows. *Geophysics*. 2012;77(3):W17-W26.

doi: 10.1190/geo2011-0336.1

17. Tan S, Huang L. An efficient finite-difference method with high-order accuracy in both time and space domains for modelling scalar-wave propagation. *Geophys J Int*. 2014;197(2):1250-1267.

doi: 10.1093/gji/ggu077

18. Tam CK, Webb JC. Dispersion-Relation-Preserving finite difference schemes for computational acoustics. *J Comput Phys*. 1993;107(2):262-281.

doi: 10.1006/jcph.1993.1142

19. Geller RJ, Takeuchi N. Optimally accurate second-order time-domain finite difference scheme for the elastic equation of motion: One-dimensional case. *Geophys J Int*. 1998;135(1):48-62.

doi: 10.1046/j.1365-246x.1998.00596.x

20. Zhang JH, Yao ZX. Optimized finite-difference operator for broadband seismic wave modeling. *Geophysics*. 2012;78(1):A13-A18.

doi: 10.1190/geo2012-0277.1

21. Zhang JH, Yao ZX. Optimized explicit finite-difference schemes for spatial derivatives using maximum norm. *J Comput Phys*. 2013;250:511-526.

doi: 10.1016/j.jcp.2013.04.029

22. Liu Y. Globally optimal finite-difference schemes based on least squares. *Geophysics*. 2013;78(4):T113-T132.

doi: 10.1190/geo2012-0480.1

23. Liu Y. Optimal staggered-grid finite-difference schemes based on least-squares for wave equation modelling. *Geophys J Int*. 2014;197(2):1033-1047.

doi: 10.1093/gji/ggu032

24. Yang L, Yan H, Liu H. Optimal implicit staggered-grid finite-difference schemes based on the sampling approximation method for seismic modelling. *Geophys Prospect*. 2015;64(3):595-610.

doi: 10.1111/1365-2478.12325

25. Miao Z, Zhang J. Simplified implicit finite-difference method of spatial derivative using explicit schemes with optimized constant coefficients based on L1 norm. *Geophysics*. 2023;89(2):T47-T59.

doi: 10.1190/geo2023-0246.1

26. Peng W, Huang J, Shen Y. Reducing the low-wavenumber dispersion error by building the Lagrange dual problem with a powerful local restriction. *J Geophys Eng*. 2023;20(4):798-815.

doi: 10.1093/jge/gxad047

27. Brekhovskikh, L.M. *Waves in Layered Media*. Vol. 42. New York: Academic Press; 1960. p. 129.

28. Manikas TW, Cain JT. *Genetic Algorithms vs. Simulated Annealing: A Comparison of Approaches for Solving the Circuit Partitioning Problem*; 1996. Available from: https://digitalrepository.smu.edu/engineering_compsci_research/1 [Last accessed on 2025 Apr 13].

29. Santos EPD, Xavier CR, Goldfeld P, Dickstein F, Santos RWD. Comparing genetic algorithms and Newton-Like methods for the solution of the history matching problem. In: *Lecture Notes in Computer Science*. Berlin: Springer; 2009. p. 377-386.

doi: 10.1007/978-3-642-01970-8_37

30. Smith, Julius O. *Physical Audio Signal Processing*. California: Stan Ford University: 2010. Available from: https://ci.nii.ac.jp/ncid/bb07079768?l=en [Last accessed on 2025 Apr 13].

31. Billette FJ, Brandsberg-Dahl S. The 2004 BP Velocity Benchmark. In: *67th EAGE Conference and Exhibition*. Bunnik: European Association of Geoscientists and Engineers; 2005.